J Mater Sci (2011) 46:1359–1368
DOI 10.1007/s10853-010-4927-0

Effects of the porcelain-fused-to-metal firing process on the surface and corrosion of two Co–Cr dental alloys

Jing Qiu · Wei-qiang Yu · Fu-qiang Zhang

Received: 14 July 2010 / Accepted: 14 September 2010 / Published online: 16 October 2010

Abstract The aim of this study was to evaluate the effects of a simulated porcelain-fused-to-metal (PFM) firing process on the surface, corrosion behavior, and cell culture response of two cobalt–chromium (Co–Cr) dental alloys. Two Co–Cr dental alloys were tested—a high and a low molybdenum (Mo)-containing alloys. Before PFM firing, as-cast alloy specimens were examined for their microstructure, surface composition, and hardness. Corrosion behavior was evaluated using electrochemical impedance spectroscopy tests. Mouse 3T3 fibroblasts were exposed indirectly to specimens and MTT cell proliferation assays were performed after 3 and 6 days. The cell culture medium exposed to specimens was analyzed for metal ion release. After firing, similar alloy specimens were examined for the same properties. The tests showed that the PFM firing changed both alloys' microstructures and hardness values. After PFM firing, the corrosion resistance of the low Mo-containing Co–Cr alloy decreased statistically, which corresponded with a reduction of Cr and oxygen levels in the surface oxides via X-ray photoelectron spectroscopy. Also, the MTT assay of this alloy decreased significantly corresponding with an obvious increase of Co release after the firing. For the high Mo-containing Co–Cr alloy, the surface composition, corrosion resistance, and cell culture response were not significantly changed after PFM firing. The results suggested that the corrosion resistance and biocompatibility of the low Mo-containing Co–Cr alloy decreased after PFM firing, whereas the firing process had little effect on the same properties of the high Mo-containing Co–Cr alloy.

J. Qiu · W. Yu · F. Zhang (✉)
Department of Prosthodontics, School of Stomatology, Ninth People's Hospital, School of Medicine, Shanghai Jiao Tong University, Shanghai Key Laboratory of Stomatology, Shanghai 200011, People's Republic of China
e-mail: fredzc@online.sh.cn

J. Qiu
Research Institute of Stomatology, College of Stomatology, Nanjing Medical University, Nanjing 210029, People's Republic of China

Introduction

For many years, clinicians have used high noble-content alloys for dental prostheses. These alloys possess compatible biological properties and good corrosion resistance [1, 2]. However, their dental applications became restricted due to the increasing cost of gold throughout the 1980's [3]. Consequently, more dental materials are studied and used [4–7]. Among them, non-precious materials such as nickel–chromium (Ni–Cr) alloys are now commonly used for the substructure of metal–ceramic restorations. When compared with the noble alloys, Ni–Cr alloys offer the advantage of an increased modulus of elasticity that allows thinner sections of the alloy to be used, and thus less sound tooth destruction during artificial crown preparation. In addition, the thermal expansion coefficient of Ni–Cr alloys is well matched to that of conventional veneering porcelain [8]. Nevertheless, doubts remain as to the biocompatibility of Ni–Cr alloys because of Ni-ion release during corrosion. Ni is the most allergenic of all metallic elements [9], and Ni sensitivity is thought to be a potential clinical effect of such dental casting alloys [10]. Because of these problems, some practitioners now prefer to use other base-metal alloys such as Co–Cr for fixed prostheses [11]. Given this new clinical use, it is important to improve our knowledge regarding the properties of Co–Cr alloys.

Dental alloys used in fixed prostheses may, for aesthetic purposes, have a porcelain veneer fired onto the cast

substructures. This type of metal-ceramic restoration is often referred to as a porcelain-fused-to-metal (PFM) restoration. In the oral environment, the corrosion resistance of dental alloys relies on a spontaneously formed surface oxide layer [12, 13]. When dental alloys are used in the fabrication of PFM restorations, often only the facial surface of the substructure is veneered, leaving the lingual and occlusal surfaces exposed, as well as the sub-gingival margins.

For clinical applications, the porcelain firing process requires high temperature cycles through four stages from 950 to 1010 °C. The procedure inevitably alters the microstructure of dental alloys in a variety of ways, including homogenization, phase transformation, and oxidation. These changes in microstructure may affect the development of protective surface oxides that would, in turn, result in changes to the corrosion resistance of the alloys. Thus, to minimize the release of alloy corrosion products into the patient's tissues from the exposed metal surfaces of PFM restorations, it is important to evaluate the effects of the porcelain firing process on the corrosion behavior of base-metal dental alloys.

Only a few studies have examined the influence of the PFM firing process on the surface and corrosion properties of base-metal alloys such as Ni–Cr. Roach et al. [14] reported that some Ni–Cr alloys had a decrease in Cr and molybdenum (Mo) content in the surface oxide and showed an increase in corrosion rate after PFM firing. A recent study of Lin et al. [15] on two Ni–Cr alloys (beryllium (Be)-free and Be-addition) found new phases in the alloys' microstructure. There were also significant increases in Ni and Mo ion release from both alloys after PFM firing. Regarding Co–Cr alloys used for fixed dental restorations, a few studies have assessed their corrosion behavior in artificial saliva [16, 17]. However, in these studies the PFM firing process was not simulated, and changes in alloy microstructure and corrosion properties were not evaluated. In fact, a search of current literature revealed no scientific evaluations of the effects of PFM firing on alloy microstructure and corrosion properties of Co–Cr alloys. Therefore, we report for the first time the effects of a simulated PFM firing process on the surface, corrosion behavior, and cell culture response of two Co–Cr dental alloys. Such information should advance the understanding of the potential clinical performance and health risks of these alloys.

Materials and methods

Materials and sample preparation

Two commercially available Co–Cr alloys routinely used for fabricating PFM restorations were evaluated, namely Wirobond C (Bego Dental, Bremen, Germany) and Starloy C (DeguDent, Hanau-Wolfgang, Germany). The Wirobond C alloy contained a high Mo content (6 wt%), while the Starloy C alloy contained a low bulk level of Mo (1 wt%). The compositions of the alloys as determined by the manufacturers are given in Table 1.

Table 1 Composition of studied alloys

Alloys	Components (wt%)					
	Co	Cr	Mo	W	Nb	Other
Wirobond C	61	26	6	5	–	Si 1, Fe 0.5, Ce 0.5
Starloy C	59.4	24.5	1	10	2	V 2, Si 1, Fe 0.1

Information supplied by the manufacturers

The samples (10 mm diameter and 3 mm thickness) were prepared by a flame casting method using an oxygen–propane gas mixture. With the use of a grinder-polisher machine (Beta, Buehler Ltd., Lake Bluff, IL, USA), the casting specimens were wet ground with silicon carbide papers and then polished with a diamond powder suspension. After that, the specimens were ultrasonically cleaned in ethanol, and finally with de-ionized water. To simulate the application of a porcelain veneer, half of all specimens, selected using a random number table, were subjected to a general PFM firing cycle, which is widely used in the fabrication of PFM restorations [14, 15, 18], under vacuum in a dental porcelain furnace (Multimat C, Dentsply Int., York, PA, USA). Briefly, the specimens were degassed at 1010 °C under vacuum holding for 5 min, opaque fired at 980 °C under vacuum and air cooled, body fired at 970 °C under vacuum and air cooled, and finally glaze fired at 980 °C and air cooled. After firing, the specimens were repolished and cleaned according to the procedures described above.

Microstructure observation

Before microstructure observation, one specimen of each alloy before and one specimen of each alloy after PFM firing were etched for 30 s at ambient temperature, with a mixture of 80% by volume of hydrochloric acid, and 20% hydrogen peroxide (H_2O_2) [17]. The microstructure of the alloys before and after PFM firing were observed using a scanning electron microscope (SEM) (Sirion 200, Philips, Eindhoven, Netherlands), and photomicrographs taken at 500×.

Surface hardness testing

Five specimens of each alloy before and after porcelain firing were assessed for Vickers microhardness values by using a microhardness tester (HXD-1000TMC, Shanghai Taiming Co. Ltd., Shanghai, PR China). All tests were conducted using a load of 50 g and 10 s contact time. The

136° diamond pyramid penetrator was used. Measurements were performed at four points around the center of each specimen, and the Vickers microhardness values were calculated.

Surface analysis

For one specimen of each alloy before and after PFM firing, X-ray photoelectron spectroscopy (XPS) was used to determine the elemental components present on the surfaces and their chemical states. XPS was performed (Axis Ultra DLD surface analysis system, Kratos Analytical, Hadano, Japan) utilizing a monochromatic Al Kα electrode at 15 kV and 150W at a 45° take-off angle. Survey and high-resolution spectra were obtained using pass energies of 160 and 40 eV, respectively. Reference binding energies of each element were obtained from the National Institute of Standards and Technology XPS Online Database. All spectral features were referenced to the binding energy of adventitious carbon (284.8 eV). Quantitative analysis of the surface composition was obtained from the peak areas and atomic sensitivity factors.

Electrochemical impedance spectroscopy corrosion test

Before testing, five specimens of each alloy before and after PFM firing were carefully mounted in self-cured epoxy resin, exposing their surfaces, and ultrasonically cleaned as described previously. Corrosion tests were performed using an electrochemical potentiostat (PARSTAT 2273, Princeton Applied Research, Oak Ridge, TN, USA) via a test cell with the mounted specimen as the working electrode, a high-purity platinum wire as the counter electrode, and Ag/AgCl as the reference electrode. Corrosion tests were performed in quintuplicate for each alloy, before and after PFM firing, in Fusayama artificial saliva solution (0.4 g/L NaCl, 0.4 g/L KCl, 0.795 g/L $CaCl_2{\cdot}2H_2O$, 0.690 g/L $NaH_2PO_4{\cdot}H_2O$, 0.005 g/L $Na_2S{\cdot}9H_2O$, 1.0 g/L urea, pH = 5.0) [13], at 37 ± 0.5 °C. Each specimen was allowed to reach open circuit potential (E_{corr}) for 2 h. The E_{corr} was recorded and then a 10 mV amplitude sine wave potential was applied through a frequency range of 1000 kHz–10 MHz. Electrochemical impedance spectroscopy (EIS) tests were implemented using the dedicated PowerSine software. The acquired data, including Nyquist plot, Bode |Z|, and Bode Phase diagrams, were analyzed and fitted using an appropriate equivalent circuit by the ZsimpWin software.

Cell culture studies

Mouse 3T3 fibroblasts maintained in the current research lab were cultured in Dulbecco's modified Eagle's medium. The cells were seeded at 1×10^4 cells/cm^2 directly onto one specimen of each alloy before and after PFM firing contained in a 24-well culture plate, and incubated at 37 °C in a 5% CO_2 humidified environment. Cell morphology was examined after 3 days, since the culture medium needed to be replaced thereby removing metal ions. The cells were fixed in 2.5% glutaraldehyde in 0.1 M sodium cacodylate for 1 h, rinsed in a buffer wash containing 0.1 M sodium cacodylate and 0.25 M sucrose at a pH of 7.3 before dehydration using an ethanol series (30, 40, 50, 70, 90, and 100%) and critical point drying from liquid CO_2 [18]. Cells were sputter coated with gold and then observed using SEM (Sirion 200, Philips, Eindhoven, Netherlands) at 500× and 1000×.

To compare the cell proliferation rates, the cells were exposed indirectly to the alloys. Three specimens of each alloy before and after PFM firing were immersed for 7 days in culture medium at 3:1 volume of solution to surface area of the specimens. The cells were then seeded at 4×10^3 cells/cm^2 into a 96-well culture plate containing the exposed medium and incubated in a 5% CO_2 humidified environment at 37 °C, replacing the culture medium after 3 days. After days 3 and 6, cell proliferation was determined using the MTT assay. MTT (3-(4,5-dimethylthiazol-2-yl)-2, 5-diphenyltetrazolium bromide) is a yellow, water-soluble tetrazolium dye that is reduced by living cells to a water-insoluble, purple formazan. Cultures were incubated with 0.5 mg/mL MTT for 4 h. Subsequently, formazan salts were dissolved with dimethylsulfoxide (DMSO), and the absorbance of each solution was measured at 590 nm in a scanning multiwell spectrophotometer (Safire^2 TECAN). All cell experimental investigations were performed in quintuplicate and compared with control cultures. Control cultures used media that had not been exposed to alloys.

The cell culture medium exposed to alloys was also analyzed for metal ion release by inductively coupled plasma atomic emission spectroscopy (ICP-AES Vista AX, Varian, Inc., Palo Alto, CA, USA) using matrix matched standards. All samples were diluted tenfold to minimize the protein and salt interference. The measurements were performed in triplicate.

Statistical analysis

Data from two Co–Cr alloys for hardness, corrosion testing, MTT, and metal ion release before and after PFM firing were statistically analyzed by SPSS 11.5 software (SPSS, Inc., Chicago, IL, USA) using standard analysis of variance (ANOVA). Student's independent samples *t*-test was used to compare differences in numerical results before and after PFM firing. The probability level for statistical significance was set at $P = 0.05$.

Results

Microstructure

The SEM micrographs of the two alloys before and after PFM firing are shown in Fig. 1. Before PFM firing, both alloys showed a solid solution matrix in a dendrite-like pattern (Fig. 1, a, c). After PFM firing, Wirobond C (the high Mo-containing Co–Cr alloy) revealed more pronounced dendritic structures with subgrains and some interdendritic precipitates in the microstructure (Fig. 1b). For Starloy C (the low Mo-containing Co–Cr alloy), the surface exhibited solute-rich interdendritic regions but revealed no significant change in microstructure after PFM firing (Fig. 1d).

Surface hardness

The Vickers microhardness values for the two alloys in both as-cast and fired conditions are shown in Fig. 2. According to the ANOVA test ($P > 0.05$), there was no significant difference between the hardness of the two alloys in both the test conditions. According to the Student's *t*-test, the hardness of Wirobond C increased significantly after PFM firing ($P < 0.01$), while the hardness of Starloy C slightly increased, but was not statistically significant ($P > 0.05$).

Surface analysis

The XPS survey spectra of Wirobond C and Starloy C are shown in Fig. 4a, b. Co, Cr, Mo, tungsten (W), and oxygen (O) were shown to be present on the alloy surfaces. From high-resolution analysis of the binding energies in Fig. 3, the O 1*s* peak exhibited a broad asymmetric shape indicating the presence of both metal oxides and hydroxides. The asymmetric peaks for all alloys of Cr 2*p* indicated the predominate presence of Cr_2O_3, and the complex peaks of Co 2*p*, Mo 3*d* and W 4*f* exhibited binding energies that correlated with the presence of metallic Co, Mo, and W as well as CoO, MoO_3, and WO_3, respectively. After PFM firing, Co 2*p* peak intensity increased on the alloy surface of Wirobond C, whereas Cr 2*p*, Mo 3*d*, O 1*s*, and W 4*f* peak intensities showed little changes (Fig. 4a). For the alloy surface of Starloy C, Cr 2*p*, and O 1*s* peak intensities decreased while Co 2*p*, Mo 3*d*, and W 4*f* peak intensities showed slight changes after PFM firing (Fig. 4b).

Figure 4c, d compares the relative composition of elements on the two alloy surfaces. For Wirobond C, the relative level of Co increased slightly after PFM firing, and levels of Cr, Mo, O, and W were very similar in both test conditions (Fig. 4c). Starloy C exhibited evident decreases in Cr and O levels and a slight increase in Co level after PFM firing (Fig. 4d).

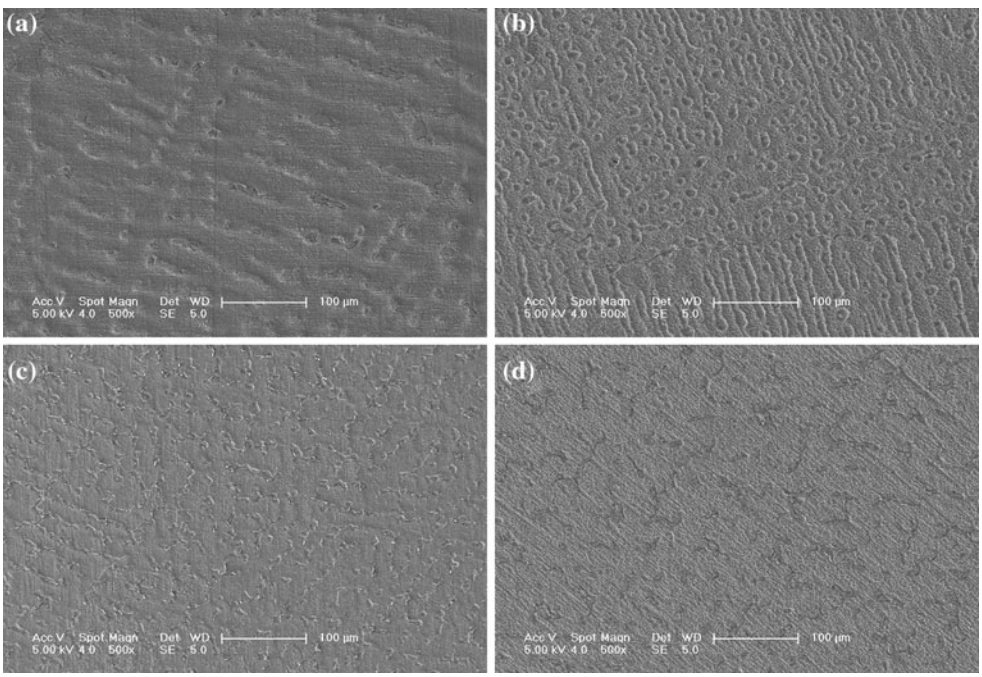

Fig. 1 SEM images of Wirobond C (the high Mo-containing Co–Cr alloy) before **a** and after **b** PFM firing (500×). Starloy C (the low Mo-containing Co–Cr alloy) before **c** and after **d** PFM firing (500×)

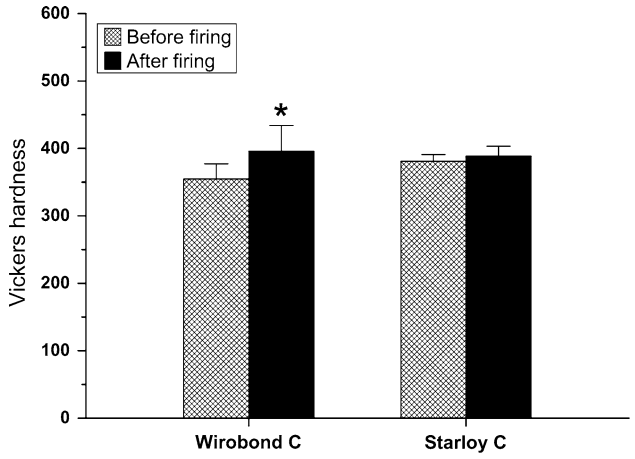

Fig. 2 Comparison of Vickers microhardness values for Wirobond C and Starloy C before and after PFM firing. *Error bars* indicate standard deviations ($n = 20$). *Asterisk* indicates a statistically significant difference for each alloy before and after firing ($P < 0.05$)

Corrosion behavior

Figure 5 presents the representative EIS data for two alloys before and after PFM firing in the form of a Nyquist plot diagram. The spectra obtained for all samples were interpreted by using an equivalent circuit model of $R_s(R_pQ)$, shown in Fig. 6, which is typical for the passive oxide layer [19, 20]. In this model, R_s represents the electrolyte resistance, R_p represents the surface oxide layer's corrosion resistance, which is inversely proportional to corrosion rate, and Q represents the constant phase elements (CPE) of the inter-barrier layer. The CPE, including Y_0 and n, represents a shift from the ideal capacitive behavior, which is due to the rough surface acquired by SiC-abrasive paper [21]. The corresponding R_p, Y_0-CPE, n, and χ^2 values are listed in Table 2. The χ^2 value within 10^{-3} indicates the excellent agreement between experimental data and fitting values. Fig. 7 shows the representative data in the form of

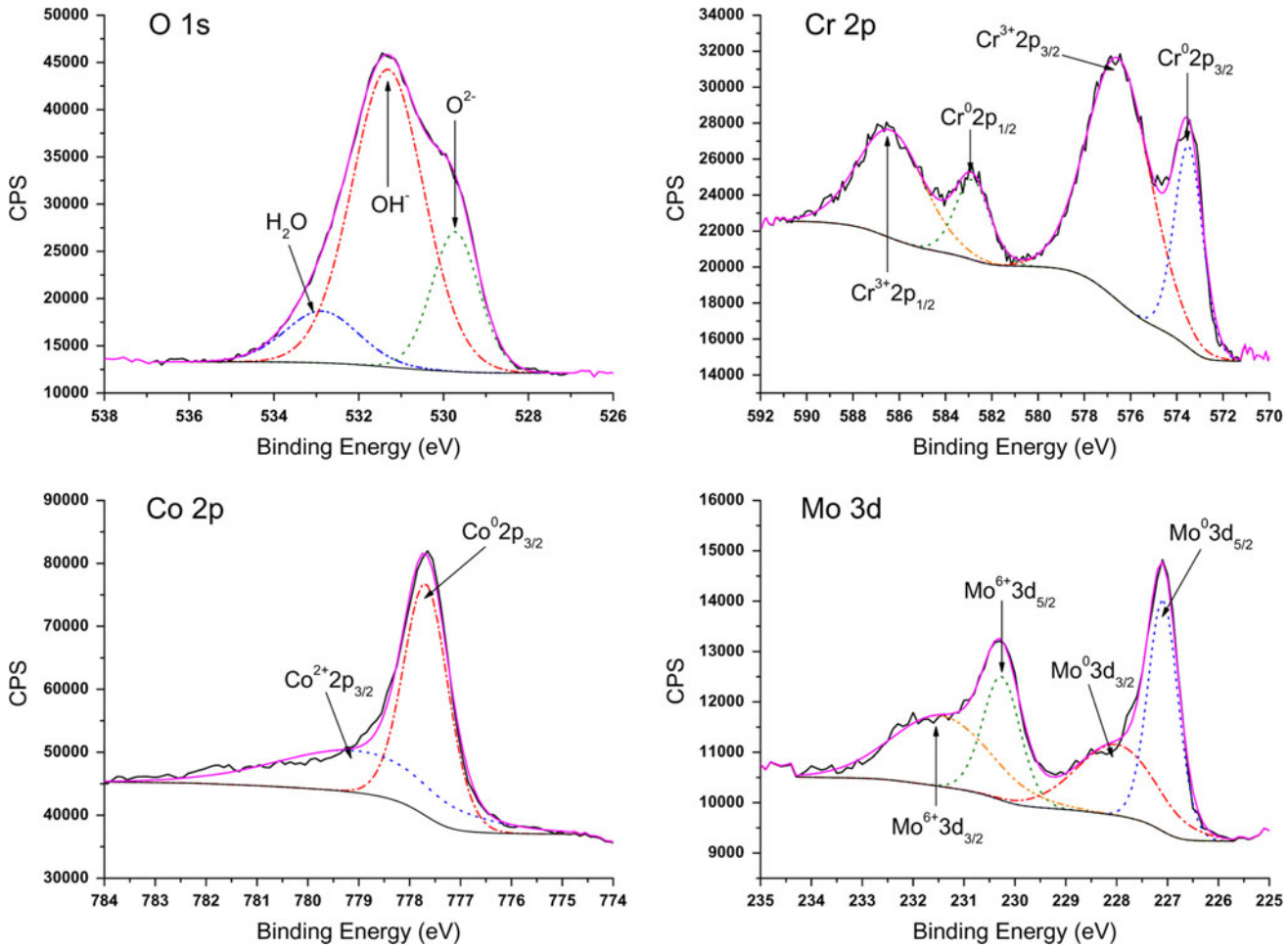

Fig. 3 Representative XPS high-resolution spectra of O 1*s*, Cr 2*p*, Co 2*p*, and Mo 3*d* for two Co–Cr alloys

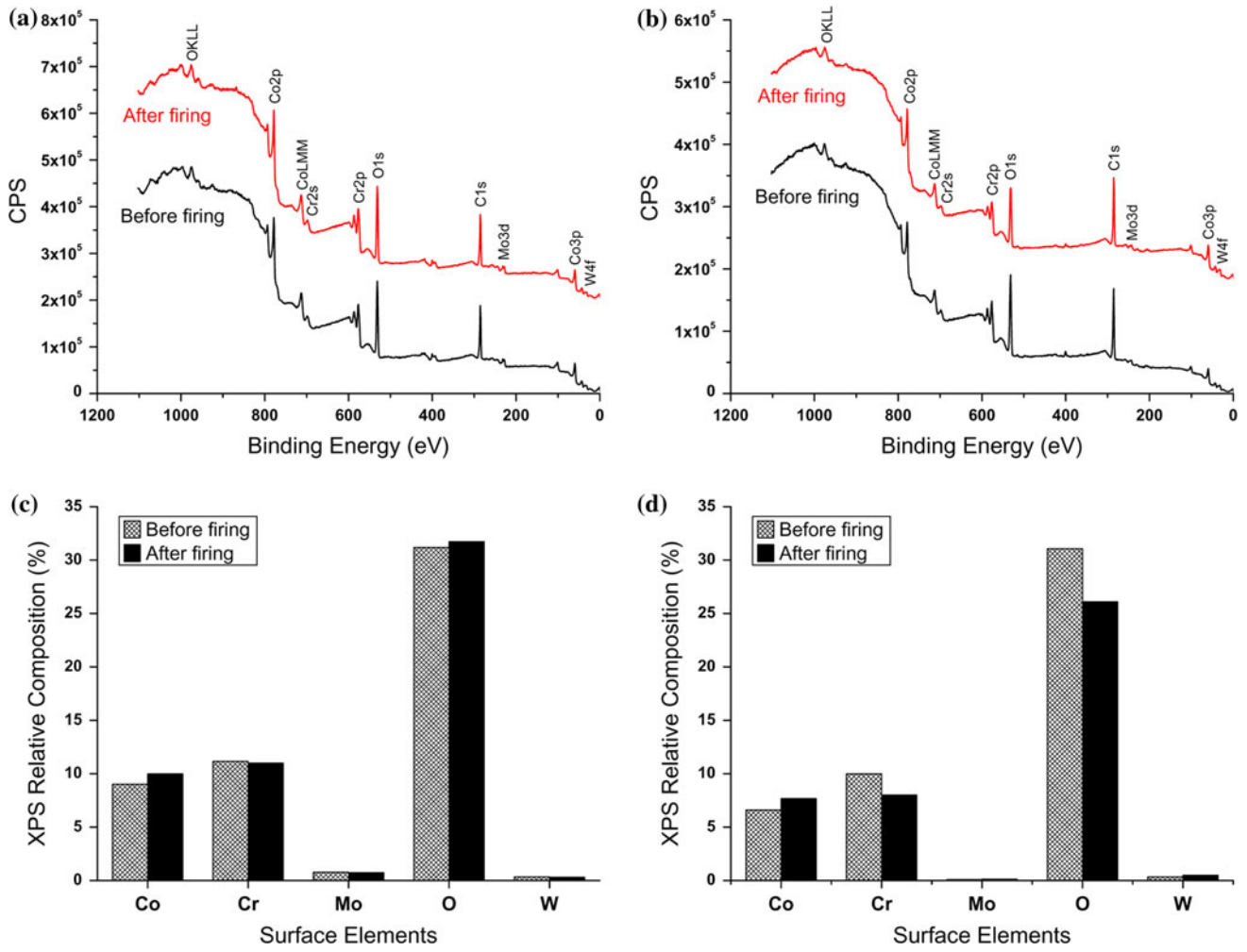

Fig. 4 The XPS survey spectra before and after PFM firing for Wirobond C **a** and Starloy C **b**. Comparison of XPS relative surface composition before and after PFM firing for Wirobond C **c** and Starloy C **d**

Bode |Z| and Bode Phase diagrams and its fitted-points by the equivalent circuit model, which were in good agreement with the experimental data. As shown in Fig. 5, all specimens approximately revealed only one semicircle. The diameter of the semicircle for Wirobond C was similar in both test conditions, while the diameter for Starloy C in the as-cast state was much larger than the one in the fired state. As listed in Table 2, according to the ANOVA test, in both test conditions, there was no significant difference of R_p value between the two Co–Cr alloys ($P > 0.05$), while Starloy C demonstrated statistically higher Y_0-CPE value compared to Wirobond C ($P = 0.02$). According to the Student's *t*-test, the values of R_p and Y_0-CPE for Wirobond C did not change statistically after PFM firing. Regarding Starloy C, the R_p value significantly decreased after PFM firing, and the value of Y_0-CPE, though not statistically significant, seemed to increase after the firing process. As shown in Fig. 7, before and after PFM firing, Wirobond C exhibited a maximum phase shift of 82.5° at 0.45 Hz and 83.0° at 1.61 Hz, while Starloy C exhibited maximum phase shift of 81.1° at 1.61 Hz and 74.1° at 10.8 Hz.

Cell culture studies

Figure 8 shows the morphology of the 3T3 fibroblasts placed on two alloys. Most areas indicated that the cells spread evenly across the alloy surface and demonstrated normal morphology. Fig. 9 shows the MTT assay of cells in cultures exposed indirectly to the two Co–Cr alloys compared with the control culture. According to the ANOVA test, after 3 and 6 days, in both test conditions, there was no significant difference between the MTT assays for the two alloys ($P > 0.05$). According to the Student's *t*-test, after 3 and 6 days, the MTT data for Wirobond C were similar in both test conditions ($P > 0.05$), whereas the PFM firing process led to a significant decrease in the MTT assay for Starloy C ($P < 0.01$). Also, a comparison of the MTT assay with the control culture revealed no statistical differences

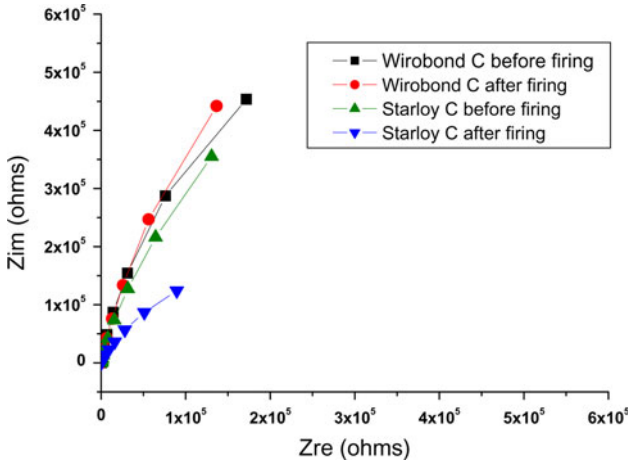

Fig. 5 The Nyquist plot diagram for two alloys before and after PFM firing

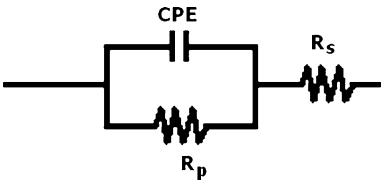

Fig. 6 Equivalent circuit, $R_s(R_pQ)$, used for fitting the experimental data

Table 2 Corrosion parameter values for the studied alloys in two test conditions

Alloys	Conditions	Impedance parameters ($n = 5$)			
		R_p	Y_0-CPE	n	χ^2
Wirobond C	As-cast	2.07 (1.37)	24.0 (5.4)	0.90 (0.01)	10^{-3}
	Fired	1.67 (1.05)	28.6 (9.1)	0.90 (0.02)	10^{-3}
Student's t-test results		$P > 0.05$	$P > 0.05$	–	–
Starloy C	As-cast	1.83 (0.37)	30.6 (1.1)	0.88 (0.02)	10^{-3}
	Fired	1.05 (0.57)	37.7 (8.8)	0.87 (0.03)	10^{-3}
Student's t-test results		$P = 0.03$*	$P > 0.05$	–	–

Values: mean (standard deviation); R_p ($M\Omega cm^{-2}$); Y_0-CPE (μFcm^{-2})

* Statistical differences ($P < 0.05$) between the as-cast and fired conditions

($P > 0.05$), except for the fired Starloy C alloy. The cultures exposed to the fired Starloy C alloy after 3 and 6 days showed a significantly lower MTT assay compared to the control culture ($P < 0.01$).

The quantity of Co ions released into the culture medium during 7 days, measured by ICP-AES, is shown in Table 3. The ion release of Cr, Mo, and W was below the detection limit for the two alloys. According to the ANOVA test, Starloy C had significantly more Co ion release compared to Wirobond C in both test conditions ($P = 0.03$). According to the Student's t-test, the cell culture medium exposed to the Starloy C alloy had significantly more Co ion release after PFM firing, while the firing process had little effect on Co ion release of the Wirobond C extract.

Discussion

Dental base-metal alloys rely on surface oxides for their corrosion resistance in the oral environment. However, few studies have addressed the effects of the high temperatures reached during PFM firing on their corrosion and surface properties. Such high temperatures may alter the composition of the surface oxides that may, in turn, alter the alloy's corrosion behavior and patient tissue reactions. In this study, the relationship between surface, corrosion behavior, and cell culture response of Co-based dental alloys have been illustrated.

After PFM firing, the XPS data of Starloy C demonstrated evident decreases in the relative amounts of Cr and O on the alloy surface compared with its as-cast condition (Fig. 4d). Results of corrosion tests show that Starloy C exhibited statistically lower R_p value after the firing. As is well known, the surface oxide layer of Co-based alloys acts as a nonconductive barrier or resistor to electron flow between the alloy and the electrolyte [22]. Several previous studies have found that the passive oxide layer developed on the Co–Cr alloy in simulated physiological solution was composed predominantly of Cr_2O_3 [23–25]. Hodgson et al. [26] also investigated the composition of the surface passive film of Co–Cr alloy in simulated biological solution by XPS. They reported that the passive film consisted mostly ($\approx$90%) of Cr_2O_3 and $Cr(OH)_3$. Cobalt was the main constituent of the alloy, but its concentration in the film was around 5%. Therefore, changes in the surface relative levels of Cr and O would change the oxide resistance of the Co-based alloys and hence their corrosion resistance. In this study, it can be concluded that, after PFM firing, the reductions in the surface relative levels of Cr and O for the Starloy C alloy resulted in a decrease in its corrosion resistance (R_p). As for Wirobond C, the XPS data exhibited little, if any, change in the relative amount of Cr and O on its surface between the as-cast and fired states (Fig. 4c). Because the surface levels of Cr and O were similar in both test conditions, it was not surprising that the R_p values for Wirobond C before and after PFM firing were statistically similar.

In this study, the corrosion test was performed using EIS. During the last decade, EIS has proven to be advantageous for the characterization of various oxide films on metal surfaces. This technique requires non-destructive procedures in the open circuit mode, i.e., neither oxidation

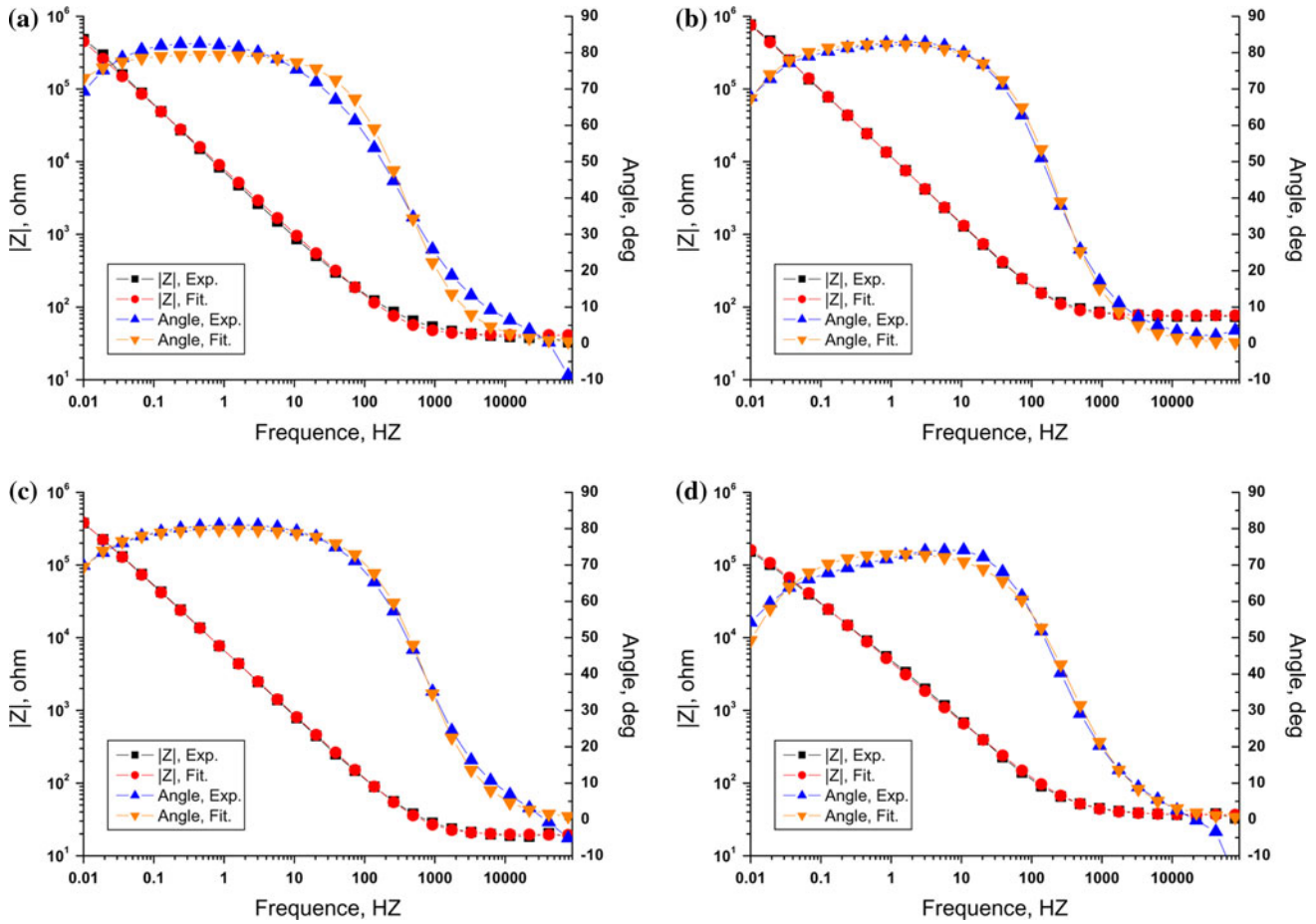

Fig. 7 Typical Bode |Z| and Bode Phase diagrams with the fitting-points by the equivalent circuit of $R_s(R_pQ)$ for Wirobond C before **a** and after **b** PFM firing, and for Starloy C before **c** and after **d** PFM firing

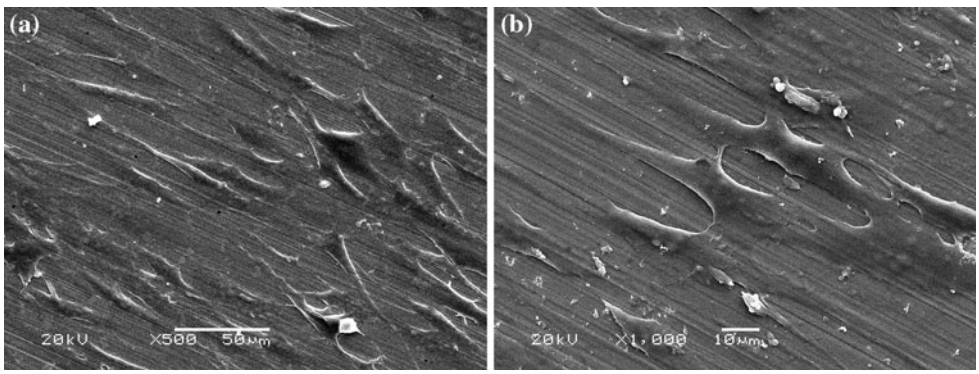

Fig. 8 SEM images showing the typical morphology of 3T3 fibroblasts on the Co–Cr alloys' surfaces by magnification of 500× **a** and 1000× **b**

nor reduction is forced to take place [27]. The Bode phase diagrams, as displayed in Fig. 7, give a clear picture of the properties of oxide films on the studied alloys' surfaces. Before PFM firing, both Co–Cr alloys showed phase angles close to 85° at medium and low frequencies. Wirobond C exhibited maximum phase shift of 82.5° at the 0.45 Hz frequency and Starloy C exhibited maximum phase shift of 81.1° at 1.61 Hz. However, after PFM firing, the Bode phase plots showed differences between the two alloys. Wirobond C exhibited phase angles close to 85° at medium and low frequencies with maximum phase shift of 83.0° at 1.61 Hz, whereas Starloy C exhibited phase angles close to 75° at a narrow range of medium frequencies with maximum phase shift of 74.1° at 10.8 Hz. Moreover, at the lowest frequency of 0.01 Hz, the phase angle of the fired Starloy C alloy dropped to about 50°, which was much lower than the as-cast Starloy C alloy. A higher phase shift at lower frequency in Bode phase plots is indicative of a

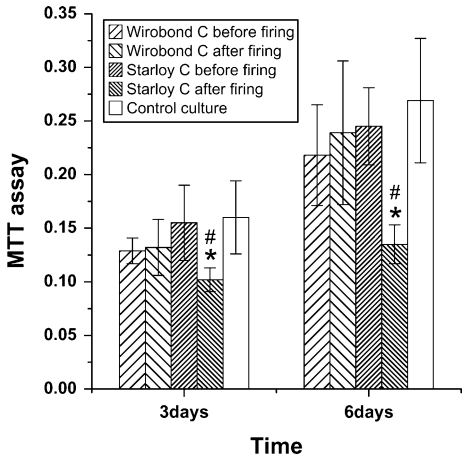

Fig. 9 The MTT assay of cells exposed indirectly to Co–Cr alloys at days 3 and 6. *Error bars* indicate standard deviations ($n = 5$), *Asterisk* indicates a statistical difference for each alloy before and after firing ($P < 0.05$), and *space* indicates a statistical difference versus the control culture ($P < 0.05$)

Table 3 Quantity of metal ion release from the studied alloys in two test conditions

Alloys	Conditions	Ion release (ppm) (Means, SD, $n = 3$)	
		Co ion	Other ions
Wirobond C	As-cast	0.34 (0.14)	Cr, Mo, and W < dl
	Fired	0.10 (0.04)	Cr, Mo, and W < dl
Student's *t*-test results		$P > 0.05$	–
Starloy C	As-cast	0.06 (0.02)	Cr, Mo, and W < dl
	Fired	4.07 (0.21)	Cr, Mo, and W < dl
Student's *t*-test results		$P < 0.01$*	–

* Statistical differences ($P < 0.05$) between the as-cast and fired conditions

dl detection limit

good passive film [28, 29]. Therefore, it was clear that the passive film formed on the Wirobond C alloy remained compact and stable in both test conditions, whereas the passive film formed on the Starloy C alloy became defective or unstable after PFM firing. The results from the Bode phase plots were also supported by the corrosion R_p values for the two alloys.

Practical experiences with Co–Cr–Mo alloys (Cr + Mo > 25 wt%) over decades show that these materials are technically, clinically, and economically excellent for dental restorations [30]. The corrosion resistance of Co-based alloys depends on the Cr and Mo contents [31]. Braemer [30] had stated that Co-based alloys compositions less than 30 wt% of Cr and Mo in total should be avoided because the corrosion rate would be too great. Starloy C had the bulk of Cr and Mo in total for 25.5 wt%, less than 30 wt%, while Wirobonc C had this bulk for 32 wt%, more than 30 wt%. According to the statement from Braemer, the corrosion rate of Starloy C would be greater than that of Wirobond C. This was confirmed by results of corrosion tests in this study, where Starloy C exhibited statistically lower R_p value and unstable passive film on its alloy surface after PFM firing. Thus, these findings show that, from the stand-point of corrosion resistance, Wirobond C should be preferred to Starloy C for clinical use of PFM restorations.

Both Wirobond C and Starloy C exhibited increases in microhardness values after PFM firing. The alteration in surface hardness might be owing to the changes in their microstructures. Before PFM firing, both alloys revealed dendrite-like structures. After the firing, Wirobond revealed more pronounced dendrite-like structure in microstructure, which corresponded with the statistically higher hardness compared to its as-cast condition. As for Starloy C, the surface exhibited solute-rich dendrite-like regions but revealed no apparent change in microstructure after the firing, which was responsible for the slightly increased hardness with no statistical difference compared to its as-cast condition. The higher microhardness values after PFM firing would make these Co–Cr alloys difficult to handle clinically.

As is well known, any metal surrounded by a biological system will corrode, leading to the release of metal ions that cause adverse physiological effects, including cytotoxicity, genotoxicity, and metal allergy [32, 33]. In this study, after PFM firing Starloy C was more susceptible to corrosion and was thus likely to release more metal ions into the environment. This was consistent with the significant increase in Co release and reduction in cell proliferation for Starloy C after firing. Regarding Wirobond C, Co ion release and cell proliferation showed no statistical changes before and after PFM firing, which also paralleled the result of its corrosion test. Beyersmann [34] reported that Co is genotoxic because it inhibited the repair of damaged DNA. When H_2O_2 was present, Co directly caused site-specific DNA damage [35]. The metal ion of Co can also lead to cell apoptosis by stimulating extrinsic and intrinsic apoptotic pathways [36, 37]. Pro-inflammatory cytokine release has been correlated with the metal ion of Co. A study by Catelas et al. found that a high amount of the cytokine tumor necrosis factor (TNF)-α was released upon exposure to a low concentration of Co ion (8–10 ppm) [38]. TNF-α is one of the primary stimuli in the inflammatory cascade [39, 40]. In this study, after PFM firing, the measured Co release of the Starloy C alloy increased reaching to more than 4 ppm. In addition, Hallab et al. [41] found that Co–Cr alloy corrosion products were immunologically reactive since it can become complexed with high molecular weight serum proteins, especially immunoglobulins. Although metal ion release into a culture medium can be relatively low, extended low dose exposures would increase the risk of cytotoxicity, genotoxicity, or metal sensitivity occurring [42, 43]. The released Co ion from Co–Cr alloys might cause the injury of cells in

adjacent oral tissues, such as human gingival fibroblasts [44]. In the oral environment, these reactions are more possibly localized to the contact zone with PFM restorations, including the sub-gingival margins, and related to oral symptoms of gingival inflammation or discoloration [10]. Furthermore, long-term oral exposure might cause increased cobalt levels in other systemic organs. Firriolo et al. [45] reported that cobalt was distributed to the largest extent in the liver and kidneys following a single oral dose of soluble cobalt to rats. Therefore, the in vivo impacts of greater Co release from the Starloy C alloy after PFM firing require further investigation.

Conclusions

The PFM firing process altered two Co–Cr alloys' microstructures and hardness. The corrosion resistance and biocompatibility of the low Mo-containing Co–Cr alloy decreased after PFM firing, whereas the firing process had little effect on the same properties of the high Mo-containing Co–Cr alloy. The increase in Co release of the low Mo-containing Co–Cr alloy after PFM firing requires further investigation before conducting in vivo studies.

Acknowledgements This work was supported by Shanghai Leading Academic Discipline Project (Project Number: S30206) and Science and Technology committee of Shanghai (08DZ2271100 and 0852nm02900).

References

1. Yilmaz B, Ozçelik TB, Wee AG (2009) J Prosthet Dent 101:395
2. Shiraishi T, Takuma Y, Fujita T, Miura E, Kunihiro H (2009) J Mater Sci 44:2796. doi:10.1007/s10853-009-3368-0
3. Leinfelder KF (1997) J Am Dent Assoc 128:37
4. Lim JI, Lim KJ, Lim HN, Lee YK (2010) J Mater Sci 45:5211. doi:10.1007/s10853-010-4560-y
5. Zhang LF, Gao Y, Chen Q, Tian M, Fong H (2010) J Mater Sci 45:2521. doi:10.1007/s10853-010-4238-5
6. Chan KS, Nicolella DP, Furman BR, Wellinghoff ST, Rawls HR, Pratsinis SE (2009) J Mater Sci 44:6117. doi:10.1007/s10853-009-3846-4
7. Karlinsey R, Mackey A (2009) J Mater Sci 44:346. doi:10.1007/s10853-008-3068-1
8. Craig RG, Powers JM (2002) Restorative dental materials, 11th edn. Mosby, St. Louis
9. Setcos JC, Babaei-Mahani A, Di Silvio L, Mjör IA, Wilson NHF (2006) Dent Mater 22:1163
10. Schmalz G, Garhammer P (2002) Dent Mater 18:396
11. Viennot S, Dalard F, Malquarti G, Grosgogeat B (2006) J Prosthet Dent 96:100
12. Huang HH (2002) J Biomed Mater Res 60:458
13. Al-Hity RR, Kappert HF, Viennot S, Dalard F, Grosgogeat B (2007) Dent Mater 23:679
14. Roach MD, Wolan JT, Parsell DE, Bumgardner JD (2000) J Prosthet Dent 84:623
15. Lin HY, Bowers B, Wolan JT, Cai Z, Bumgardner JD (2008) Dent Mater 24:378
16. Mareci D, Nemtoi G, Aelenei N, Bocanu C (2005) Eur Cell Mater 10:1
17. Viennot S, Dalard F, Lissac M, Grosgogeat B (2005) Eur J Oral Sci 113:90
18. Wylie CM, Shelton RM, Fleming GJ, Davenport AJ (2007) Dent Mater 23:714
19. Viswanathan SS, Han-Cheol C (2009) Trans Nonferrous Met Soc China 19:785
20. Oliveira NT, Guastaldi AC (2009) Acta Biomater 5:399
21. Aparicio C, Gil FJ, Fonseca C, Barbosa M, Planell JA (2003) Biomaterials 24:263
22. Metikos-Huković M, Pilić Z, Babić R, Omanović D (2006) Acta Biomater 2:693
23. Hanawa T, Hiromoto S, Asami K (2001) Appl Surf Sci 183:68
24. Milosev I, Strehblow H-H (2003) Electrochim Acta 48:2767
25. Kocijan A, Milosev I, Pihlar B (2004) J Mater Sci Mater Med 15:643
26. Hodgson AWE, Kurz S, Virtanen S, Fervel V, Olsson COA, Mischler S (2004) Electrochim Acta 49:2167
27. Hamdy AS, El-Shenawy E, El-Bitar T (2006) Int J Electrochem Sci 1:171
28. Kalman E, Varhegyi B, Bako I, Felhosi I, Karman FH, Shaban A (1994) J Electrochem Soc 141:3357
29. Sharma M, Kumar AV, Singh N (2008) J Mater Sci Mater Med 19:2647
30. Braemer W (2001) Adv Eng Mater 3:753
31. Matkovic T, Matkovic P, Malina J (2004) J Alloys Compd 366:293
32. Hallab N, Merritt K, Jacobs JJ (2001) J Bone Joint Surg Am 83:428
33. Sargeant A, Goswami T (2007) Mater Des 28:155
34. Beyersmann D (2002) Toxicol Lett 127:63
35. Kawanishi S, Hiraku Y, Murata M, Oikawa S (2002) Free Radic Biol Med 32:822
36. Pulido M, Parrish A (2003) Mutat Res 533:227
37. De Boeck M, Kirsch-Volders M, Lison D (2003) Mutat Res 533:135
38. Catelas I, Petit A, Zukor DJ, Antoniou J, Huk OL (2003) Biomaterials 24:383
39. Galley HF, Webster NR (1996) Br J Anaesth 77:11
40. Cunha TM, Verri WA Jr, Silva JS, Poole S, Cunha FQ, Ferreira SH (2005) Proc Natl Acad Sci USA 102:1755
41. Hallab N, Mikecz K, Vermes C, Skipor A, Jacobs J (2001) Mol Cell Biochem 222:127
42. Wataha JC, Nelson KS, Lockwood PE (2001) Dent Mater 17:409
43. Wataha JC, Lockwood PE, Schedle A, Noda M, Bouillaguet S (2002) J Oral Rehabil 29:133
44. Issa Y, Brunton P, Waters CM, Watts DC (2008) Dent Mater 24:281
45. Firriolo JM, Ayala-Fierro F, Sipes IG, Carter DE (1999) J Toxicol Environ Health A 58:383